Prognosis Related to Metastatic Burden Measured by ^{18}F-Fluorocholine PET/CT in Castration-Resistant Prostate Cancer

Sandi A. Kwee[1–3], John Lim[1,2], Alex Watanabe[1], Kathleen Kromer-Baker[1], and Marc N. Coel[1,2]

[1]The Queen's Medical Center, Honolulu, Hawaii; [2]Hamamatsu/Queen's PET Imaging Center, Honolulu, Hawaii; and [3]John A. Burns School of Medicine, University of Hawaii, Honolulu, Hawaii

This study investigated the prognostic significance of metabolically active tumor volume (MATV) measurements applied to ^{18}F-fluorocholine PET/CT in castration-resistant prostate cancer (CRPC). **Methods:** ^{18}F-fluorocholine PET/CT imaging was performed on 30 patients with CRPC. Metastatic disease was quantified on the basis of maximum standardized uptake value (SUV_{max}), MATV, and total lesion activity (TLA = MATV × mean standardized uptake value). Tumor burden indices derived from whole-body summation of PET tumor volume measurements (i.e., net MATV and net TLA) were evaluated as variables in Cox regression and Kaplan–Meier survival analyses. **Results:** Net MATV ranged from 0.12 cm^3 to 1,543.9 cm^3 (median, 52.6 cm^3). Net TLA ranged from 0.40 to 6,688.7 g (median, 225.1 g). Prostate-specific antigen level at the time of PET correlated significantly with net MATV (Pearson $r = 0.65$, $P = 0.0001$) and net TLA ($r = 0.60$, $P = 0.0005$) but not highest lesional SUV_{max} of each scan. Survivors were followed for a median 23 mo (range, 6–38 mo). On Cox regression analyses, overall survival had a significant association with net MATV ($P = 0.0068$), net TLA ($P = 0.0072$), and highest lesion SUV_{max} ($P = 0.0173$) and a borderline association with prostate-specific antigen level ($P = 0.0458$). Only net MATV and net TLA remained significant in univariate-adjusted survival analyses. Kaplan–Meier analysis demonstrated significant differences in survival between groups stratified by median net MATV (log-rank $P = 0.0371$), net TLA (log-rank $P = 0.0371$), and highest lesion SUV_{max} (log-rank $P = 0.0223$). **Conclusion:** Metastatic prostate cancer detected by ^{18}F-fluorocholine PET/CT can be quantified on the basis of volumetric measurements of tumor metabolic activity. The prognostic value of ^{18}F-fluorocholine PET/CT may stem from this capacity to assess whole-body tumor burden. With further clinical validation, ^{18}F-fluorocholine PET-based indices of global disease activity and mortality risk could prove useful in patient-individualized treatment of CRPC.

Key Words: castrate resistant prostate cancer; positron emission tomography; fluorocholine; survival

J Nucl Med 2014; 55:905–910
DOI: 10.2967/jnumed.113.135194

In men, prostate cancer is the second leading cause of cancer death after lung cancer (*1*). In industrialized parts of the world, deaths from prostate cancer often stem from metastases that have arisen in the setting of castration-resistant prostate cancer (CRPC). Beginning with docetaxel-based chemotherapy in 2004, several therapeutic agents are now available to improve survival in CRPC (*2–4*). However, the optimal sequencing of these various treatments has not yet been resolved, in part because of the scarcity of prognostic markers for deciding clinical management on the basis of disease manifestation. Patient-individualized treatment of CRPC may hinge on developing better biomarkers, since rates of clinical progression and therapeutic response can vary considerably in patients with this diagnosis (*5*). Unfortunately, conventional diagnostic imaging and prostate-specific antigen (PSA) testing have shown limited value as prognostic markers for advanced prostate cancer (*6*). And while predictive nomograms have been developed for CRPC (*7,8*), they provide little information relevant to tumor biology. Consequently, there is continued interest in tumor markers that can be applied to predictively characterize the clinical progression of advanced prostate cancer.

^{18}F-fluorocholine is a PET agent based on choline that can be used to detect metastatic prostate cancer (*9–11*). Although the utility of ^{18}F-fluorocholine PET/CT for localizing metastatic prostate cancer is supported by studies from multiple institutions (*9,11*), data on the clinical prognostic significance of the metabolic information provided by ^{18}F-fluorocholine PET/CT remain sparse. In contrast, prognostic indices have been developed and successfully applied to clinical ^{18}F-FDG PET/CT studies in a variety of cancers. Tumor indices based on measuring the metabolically active tumor volume (MATV) in particular have shown much greater prognostic value than conventional PET measurements such as the maximum standardized uptake value (SUV_{max}) (*12–14*).

Because MATV measurements can be applied to each individual metastasis that is detected, it is reasoned that summing together these measurements may provide a global estimate of metastatic burden for each patient imaged by ^{18}F-fluorocholine PET/CT. To explore the prognostic value of gauging the extent of metastatic disease in this way, we conducted a prospective study investigating the relationship between metabolic tumor volume on whole-body ^{18}F-fluorocholine PET/CT and overall survival (OS) in patients with prostate cancer that has become resistant to complete androgen blockade.

MATERIALS AND METHODS

Patients

Patients with CRPC were prospectively recruited from institutional and community oncology practices from August 2009 to February 2012. Study eligibility criteria were age over 18 y, prostate cancer treated by definitive surgery or radiotherapy, CRPC as defined by 2 rising PSA measurements of 2.0 ng/mL or higher while on complete

Received Nov. 14, 2013; revision accepted Jan. 1, 2014.
For correspondence or reprints contact: Sandi A. Kwee, The Queen's Medical Center, 1301 Punchbowl St., Honolulu, HI 96813.
E-mail: skwee@queens.org
Published online Mar. 27, 2014.

androgen blockade for longer than 3 mo, and clinical life expectancy of more than 12 wk (*5*). Patients with other malignancies diagnosed in the past 3 y were excluded.

This was an institutional review board–approved study, and written informed consent was obtained from all patients. A medical oncologist selected all treatments independently of the study. Treatments were recorded as potential variables in survival analysis. Censored survival data were measured as months from the date of PET imaging to the date of death from any cause or the date of last clinical follow-up.

Radiopharmaceutical Synthesis

^{18}F was produced using an 11-MeV self-shielded automated cyclotron (RDS 111; Siemens Medical Solutions). ^{18}F-fluorocholine synthesis was performed by fluorination of ditosylmethane with ^{18}F followed by alkylation of the intermediate with dimethylethanolamine using a standard chemical process control unit (CPCU; CTI/Siemens) (*15*). All products passed standard assays for radiochemical purity, radionuclidic identity, chemical purity, and nonpyrogenicity before injection. Final radiochemical purity was 99%.

PET/CT Imaging

All patients refrained from eating and drinking for at least 3 h before undergoing PET/CT. A Gemini TF-64 PET/CT scanner (Philips Healthcare) was used to obtain the images. First, a CT transmission scan was obtained from the pelvis to the skull with the patient supine. No intravenous contrast material was used for CT. The 64-channel helical CT scanning parameters were 120 kV, 50 mA/slice, a rotation time of 0.75 s, and a slice thickness and interval of 5.0 mm. At 12–15 min after the intravenous injection of a 2.6 MBq/kg (0.07 mCi/kg) dose of ^{18}F-fluorocholine, emission scans were acquired from the mid thigh to the skull at 2 min per bed position. PET images were reconstructed using maximum-likelihood expectation maximization with manufacturer-recommended settings. CT data were used for attenuation correction.

Image Analysis

PET/CT images were analyzed using a multimodality imaging workstation (Hybrid PDR, version 1.4c; Hermes Medical Solutions). Tumor lesions on whole-body PET/CT images were identified by a consensus of 3 readers, with 2 having significant experience in ^{18}F-fluorocholine PET/CT imaging of prostate cancer. Lesions were defined as areas of increased ^{18}F-fluorocholine uptake localized to a soft-tissue organ, lymph node, or skeletal structure with an SUV_{max} of 3.0 or greater (exceeding 2 SDs above the normal-marrow SUV). SUV was calculated as measured voxel activity divided by injected radioactivity normalized by body weight.

The MATV for each lesion was computed using a vendor-supplied segmentation algorithm by which the voxel corresponding to the SUV_{max} of the lesion was identified and a volume of interest was generated consisting of all spatially connected voxels within a fixed threshold of 40% of the SUV_{max}. A measure of the activity distribution within the volume, termed total lesion activity (TLA), was also calculated as the product of lesion mean standardized uptake value and MATV. Each patient was then assigned indices of whole-body tumor burden defined as the sum of all MATVs (net MATV) and the sum of all TLAs (net TLA) from each ^{18}F-fluorocholine PET/CT scan.

Statistical Analysis

Longitudinal clinical follow-up was used to assess OS as the primary endpoint. Univariate Cox regression assessed the significance of individual variables in relation to OS. The variables included in the analysis were age, baseline PSA (measured at the time of PET), type of subsequent treatment for CRPC, the highest lesion SUV_{max} from each scan, tumor distribution, net MATV, and net TLA. All continuous variables were examined for normality. Significantly skewed variables were log-transformed before survival analysis.

Multivariate analysis was performed to assess the effects of individual variables on OS while controlling for another variable. Multivariate analysis included only variables that were significant by univariate analysis and was limited to one adjustment based on the number of outcome events. Although age was not significant in univariate analysis, survival was analyzed with and without age adjustment because of the study demographics.

For Kaplan–Meier analysis, patients were stratified by the median values of each significant univariate predictor. Differences between survival patterns were tested for significance using the log-rank test. Correlations were assessed using Pearson correlation. Means were compared by *t* testing or ANOVA as appropriate. A probability of less than 0.05 was considered statistically significant. All statistical tests were 2-sided and performed using SAS 9.4 (SAS Institute Inc.) and MedCalc 12.5 (MedCalc Software).

RESULTS

Patients and Clinical Outcome

Median age at enrollment was 73 y (range, 54–86 y). Median PSA at the time of PET imaging was 35.1 ng/mL (range, 2.0–11,474 ng/mL). Subsequent treatments included chemotherapy (n = 11), alternate androgen/second-line hormonal therapy (n = 13), and therapeutic antiandrogen withdrawal (n = 6). The average time to initiating a subsequent treatment for CRPC after ^{18}F-fluorocholine PET/CT was 6 d (range, 1–31 d). There were no significant differences in age, PSA level, highest tumor SUV_{max}, net MATV, or net TLA between the patients receiving chemotherapy, secondary antiandrogen/hormonal therapy, or antiandrogen withdrawal (Table 1). Ten patients died during the follow-up period. The median follow-up interval in survivors was 23 mo (range, 6–38 mo).

TABLE 1
Mean Patient Characteristics by Type of Subsequent Treatment Given

Variable	All patients (n = 30)	Treatments received subsequent to PET: Withdrawal of AA (n = 6)	Chemotherapy (n = 11)	Second-line hormonal (n = 13)	ANOVA P for differences across treatment
Age	72.7	76.8	72.5	71.0	0.4003
PSA (ng/mL)	565.5	25.7	448.9	913.3	0.7082
Highest tumor SUV_{max}	7.9	6.6	8.5	8.1	0.5457
Net MATV (cm^3)	257.4	314.1	243.4	243.1	0.9332
Net TLA (g)	1,212.8	1,549.7	1,205.1	1,063.7	0.8827

AA = antiandrogen.

PET Imaging Findings

At least one ^{18}F-fluorocholine–avid lesion was found in each patient. Areas of abnormal ^{18}F-fluorocholine uptake involved only the skeletal system in 19 patients, only the lymph nodes in 5 patients, and both systems in 6 patients (Figs. 1 and 2). No soft-tissue lesions other than lymph nodes were noted. An absence of prostatic lesions was consistent with all patients having undergone primary treatment for prostate cancer.

Median net MATV was 52.6 cm^3 (range, 0.12–1,543.9 cm^3). Median net TLA was 225.1 g (range, 0.40–6,688.7 g). The median of the highest tumor SUV_{max} was 7.4 (range, 2.9–15.7). Net MATV correlated significantly with the PSA level obtained at the time of PET (Pearson $r = 0.65$, $P = 0.0001$) as well as highest tumor SUV_{max} ($r = 0.422$, $P = 0.0202$). Net TLA was also significantly correlated with PSA ($r = 0.60$, $P = 0.0005$) and highest tumor SUV_{max} ($r = 0.45$, $P = 0.0124$). Not unexpectedly, MATV and TLA were highly correlated ($r = 0.99$, $P < 0.0001$) (Fig. 3). However, there was no significant correlation between PSA and highest tumor SUV_{max} ($r = 0.11$, $P = 0.5489$).

Univariate Analysis

PSA, net MATV, and net TLA measurements required log transformation to achieve a more normal distribution before survival analysis (Fig. 4). As indicated in Table 2, highest tumor SUV_{max}, net MATV, and net TLA were significantly associated with poor OS. Differences in OS were not significantly associated with age, subsequent type of treatment, or distribution of metastatic disease as depicted on ^{18}F-fluorocholine PET/CT (i.e., lymphatic, skeletal, or both). A borderline-significant association between OS and PSA level was noted. The interval between PET scanning and treatment initiation was not associated with significant differences in OS.

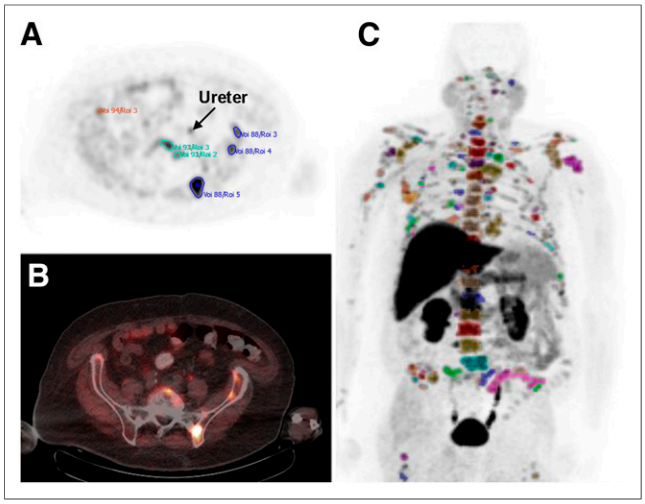

FIGURE 2. (A) Transaxial PET image through pelvis shows MATV regions (colored contours) defined around areas of increased ^{18}F-fluorocholine uptake. Because ureter contains excreted ^{18}F-fluorocholine (arrow), careful image interpretation is needed to avoid confusing it with lymph node. (B) Areas of increased ^{18}F-fluorocholine uptake delineated on previous figure correspond to sacral and iliac bone lesions on PET/CT. (C) Volume-rendered PET image shows extensive metastatic disease as defined by whole-body MATV segmentation (colored contours). Note that color on this image indicates MATV boundaries and not intensity of ^{18}F-fluorocholine uptake. These individual MATVs were summed together to provide global PET indices of metastatic burden in this study.

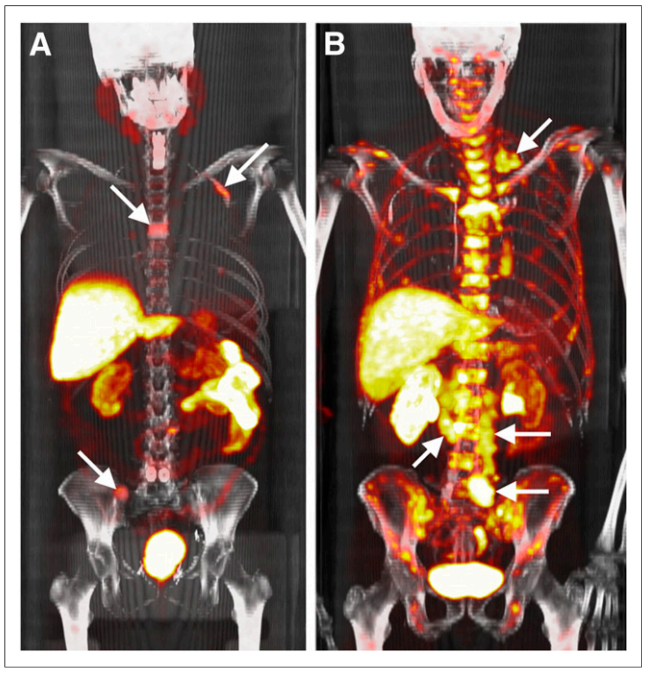

FIGURE 1. ^{18}F-fluorocholine PET/CT of CRPC. (A) Areas of increased ^{18}F-fluorocholine uptake corresponding to lesions in thoracic spine, ribs, and iliac bone (arrows) are shown on this maximum-intensity-projection PET/CT image. Net MATV was 54.7 cm^3, and net TLA was 227.6 g. PSA level was 4.9 ng/mL in this patient with relatively low tumor burden. (B) In contrast, ^{18}F-fluorocholine PET/CT from patient with PSA level of 28.1 ng/mL shows numerous areas of increased ^{18}F-fluorocholine uptake in skeleton along with lymph nodes (arrows) in left supraclavicular fossa, retroperitoneum, and pelvis. Net MATV was 924.2 cm^3, and net TLA was 4,850.0 g.

Multivariate Analysis

The results of age-adjusted Cox regression survival analysis are summarized in Table 3. Thus, PSA level, highest tumor SUV_{max}, net MATV, and net TLA remained significant factors on OS after adjusting for age.

A limited multivariate analysis involving single-parameter adjustments was performed specifically to explore the relationship between significant univariate variables. Controlling for net MATV mitigated the significance of PSA ($P = 0.8044$) and highest tumor SUV_{max} ($P = 0.7038$). Controlling for net TLA also mitigated the significance of PSA ($P = 0.7813$) and highest tumor SUV_{max} ($P = 0.7739$). In contrast, net MATV (hazard ratio [HR], 1.97; 95% confidence interval [CI], 1.15–3.38; $P = 0.0142$), net TLA (HR, 1.88; 95% CI, 1.14–3.13; $P = 0.0147$), and highest tumor SUV_{max} (HR, 1.29; 95% CI, 1.03–1.61; $P = 0.0261$) remained significant after controlling for PSA level. Finally, controlling for highest tumor SUV_{max} maintained the significance of net MATV (HR, 1.87; 95% CI, 1.01–3.46; $P = 0.0460$) and net TLA (HR, 1.83; 95% CI, 1.01–3.30; $P = 0.0471$) but not PSA level ($P = 0.0680$).

The survival curves from Kaplan–Meier analysis are shown in Figure 5. There were significant differences in survival among patients stratified by the median values of SUV_{max} of the most active tumor (log-rank $P = 0.0223$), net MATV (log rank $P = 0.0371$), and net TLA (log-rank $P = 0.0371$). In contrast, the difference in survival between groups stratified by median PSA level was borderline-insignificant (log-rank $P = 0.0531$).

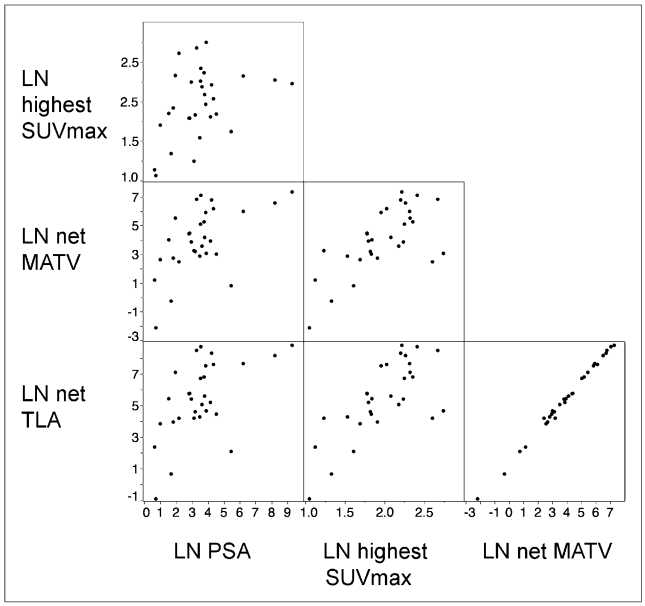

FIGURE 3. Scatterplot matrix showing relationships between significant variables. LN = natural logarithm.

DISCUSSION

Metastatic prostate cancer most commonly manifests in the bones and lymph nodes. ^{18}F-fluorocholine PET/CT can readily interrogate these areas to delineate the route and extent of metastatic progression (*9–11*). In this study, metabolic tumor volume analysis succeeded in quantifying metastatic disease found on ^{18}F-fluorocholine PET/CT in a manner that relates with prognosis. Specifically, whole-body tumor burden indices based on quantifying net MATV and net TLA on ^{18}F-fluorocholine PET/CT were found to be predictive of OS in univariate and individually adjusted Cox regression analyses. This association between metastatic burden and prognosis is well supported by other lines of research linking a heavy tumor load with increased risks of hematologic and skeleton-related complications as well as higher mortality in metastatic prostate cancer (*7,8,16–18*).

Increased choline metabolism by tumors is associated with increases in phospholipid membrane synthesis and cell proliferation (*19,20*), as well as upregulated second-messenger activity along mitogenic pathways (*21,22*). Clinical and experimental observations have also linked increased choline metabolism to biologic aggressiveness in prostate cancer (*23,24*). The results of this study also support a role for choline metabolism in promoting prostate cancer progression through the observation that the highest tumor SUV_{max} from each scan was a significant predictor of OS. Although adjustments for tumor volume abrogated the statistical significance of SUV_{max}, the biologic significance of choline metabolism cannot be entirely dismissed since lesion MATV is also defined on the basis of tumor ^{18}F-fluorocholine avidity. The biologic and prognostic implications of upregulated choline metabolism in prostate cancer should be better understood with more research.

TLA as defined in this study was based on the concept of total lesion glycolysis borrowed from ^{18}F-FDG PET studies (*12*). TLA and total lesion glycolysis build on the concept of MATV by further integrating the metabolic information with volume data. In this study, net MATV and net TLA were the only parameters found to have preserved significance after adjustment by another significant univariate. Although multivariate analyses in this study were limited to only singular adjustments because of the relatively small sample size, this preliminary observation does support metabolic volume measurements on ^{18}F-fluorocholine PET as prognostic factors that may be independent of PSA.

In this study, net MATV and net TLA measurements proved strongly colinear, suggesting that these parameters may have similar behavior in characterizing prognosis. In contrast, studies using ^{18}F-FDG PET have reported significant differences in the predictive ability of MATV and total lesion glycolysis (*25,26*). Thus, the relative predictive value of ^{18}F-fluorocholine–derived MATV and TLA in other clinical contexts, such as the measurement of therapeutic response, remains open to further study.

Patients were enrolled to this study after developing resistance to complete androgen blockade as evidenced by their rising PSA levels. All patients subsequently underwent chemotherapy or further manipulation of their androgen hormonal axis, as these were the most common treatment interventions for CRPC at the time of the study (*3,4,27*). Because treatments were selected on a clinical basis, they were not uniform in the study and therefore constitute potential confounders. However, the type of treatment received by patients did not demonstrate a significant effect on OS on Cox regression analysis, and there were no significant differences in PSA level, SUV_{max}, net MATV, or net TLA across different treatments. It is possible that any effect of treatment on survival was relatively small (e.g., docetaxel improves median survival by less than 2.5 mo (*2,3*)) or not significantly different between the types of treatment. Although it may have been possible to assess progression-free survival, OS was the only endpoint used in this study because of recognized inconsistencies in measuring progression-free survival in CRPC (*5,28*). As novel treatments for CRPC continue to emerge, their effects may warrant characterization on the basis of ^{18}F-fluorocholine PET/CT in consideration of further developing ^{18}F-fluorocholine PET/CT as a predictive biomarker for prostate cancer.

No survival differences were found related to the distribution of metastatic lesions (i.e., skeletal vs. nodal). However, the number of cases of nonskeletal metastases in this study was too small to afford a statistical conclusion. Previous studies have measured prognosis with imaging of just skeletal tumor burden (*16–18*). One study also linked poor survival with visceral disease (*8*). Further

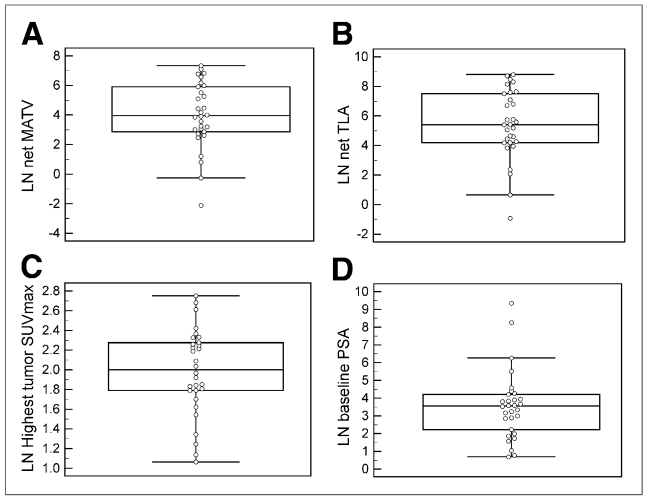

FIGURE 4. Distribution of normalized variables. Box and whisker plots show range and distribution of net MATV (A), net TLA (B), highest tumor SUV_{max} (C), and PSA (D) after normalization by natural logarithm (LN).

TABLE 2
Univariate Cox Proportional Hazards Regression Results

Variable	HR	HR 95% CI	*P*
Age	1.08	0.99–1.17	0.0896
PSA level*	1.34	1.01–1.77	0.0458
Highest tumor SUV_{max}	1.26	1.04–1.52	0.0173
Net MATV*	2.02	1.22–3.34	0.0068
Net TLA*	1.93	1.20–3.10	0.0072
Treatment (relative to AA withdrawal)			
Chemotherapy	0.38	0.08–1.73	0.2108
Second-line AA/hormonal therapy	0.65	0.13–3.22	0.5970
Metastatic disease pattern (relative to both)			
Lymphatic	1.88	0.31–11.49	0.4950
Skeletal	0.82	0.16–4.21	0.8105

*Lognormalized.
AA = antiandrogen.

research is needed to clarify the impact of lesion distribution on prognosis in metastatic CRPC.

The process of defining MATV was automated in this study to provide reproducible PET measurements with little effort. However, only one specific method of image segmentation was used, and the optimal method for defining MATVs on ^{18}F-fluorocholine PET/CT has yet to be determined. Although there are multiple approaches to PET volume segmentation (*14*), the high contrast achieved by metastases on ^{18}F-fluorocholine PET/CT made it feasible to use a relatively simple threshold-based method. Unlike with ^{18}F-FDG, the rapid clearance of ^{18}F-fluorocholine from the vascular pool allowed PET images to be acquired shortly after tracer injection while still achieving good image quality and background contrast for automated MATV segmentation. Nonetheless, it may be worthwhile to further develop MATV segmentation methods specifically for ^{18}F-fluorocholine PET/CT based on the potential clinical applications for such a technique.

The main limitations of this study were its sample size and single-institution setting. Both SUV_{max} and MATV are nonabsolute measures that are influenced by factors such as PET scanner calibration and image reconstruction method. The timing of tracer administration and image acquisition may also affect measurement reproducibility. Further research is required to characterize these effects and their impact on tumor volume segmentation on ^{18}F-fluorocholine PET/CT. Consequently, parameters from this study may not necessarily be optimal for other institutions, and further work will be required to validate and generalize this technique for the clinical setting.

Because biopsies to confirm metastatic prostate cancer are often not clinically warranted, histopathologic diagnoses were not used to confirm the tumor origin of lesions detected by ^{18}F-fluorocholine PET/CT. Thus, an assumption that the lesions quantified in this study were indeed prostate cancer metastases was applied. Hopefully, the study eligibility criteria minimized the possibility that another disease process produced ^{18}F-fluorocholine–avid lesions, and given that all patients met the criteria for advanced prostate cancer at enrollment, this limitation should not significantly detract from the study conclusions.

Baseline prognostic markers are important in clinical trials to establish cohorts of uniform prognosis before randomization. They are also crucial in clinical practice to help in tailoring treatments to overall risk. Previous efforts in prostate cancer risk assessment have so far led to the development of clinical predictive nomograms (*7,8*). Although such nomograms tell little about the tumors directly, their incorporation of hemoglobin, lactate dehydrogenase, and alkaline phosphatase levels does serve to reflect the degree of skeletal and marrow compromise resulting from metastatic disease. Because PET can provide more direct information about the tumor, this imaging technique could complement existing prognostic markers, or at least provide unique information to enhance future predictive nomograms. Thus, further validation of ^{18}F-fluorocholine PET/CT as a prognostic marker should ideally be pursued in the context of existing prognostic tools.

Although the diagnostic sensitivity and specificity of ^{18}F-fluorocholine PET/CT for detecting CRPC is reportedly superior to that of conventional imaging (*29*), it is possible that some metastases may not be detected solely on the basis of increased ^{18}F-fluorocholine uptake. With regard to disease detectability, the results of the current study suggest that having only a small volume of disease found on ^{18}F-fluorocholine PET/CT can impart a favorable prognosis even in patients with CRPC. The natural history of prostate cancer progression is complex, and the diagnostic sensitivity of ^{18}F-fluorocholine PET/CT may vary depending on prior treatments and clinical circumstance (*9*). The prognostic significance of a "negative" result on ^{18}F-fluorocholine PET/CT is unknown in clinical states such as biochemical recurrence, evolving hormone resistance, or even initially when deciding on the primary treatment. Because treatment decisions throughout the course of prostate cancer are often predicated on considerations of competing mortality risks, it may be worthwhile to further explore the prognostic value of ^{18}F-fluorocholine PET/CT in clinical situations in which this technique has already been applied for disease detection.

TABLE 3
Age-Adjusted Cox Proportional Hazards Regression Results

Variable	HR	HR 95% CI	*P*
PSA level*	1.40	1.04–1.88	0.0259
Highest tumor SUV_{max}	1.29	1.07–1.55	0.0088
Net MATV*	1.97	1.20–3.24	0.0077
Net TLA*	1.91	1.19–3.05	0.0072

*Lognormalized.

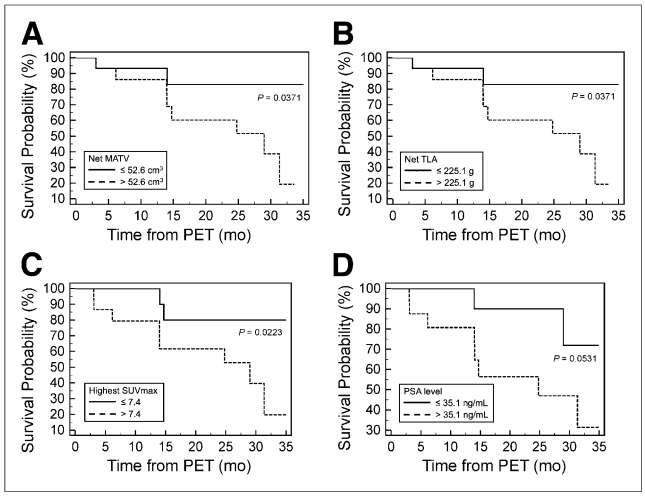

FIGURE 5. Kaplan–Meier survival curves. Differences in survival were significant among patients stratified by net MATV (A), net TLA (B), and SUV_{max} of most active tumor (C) and borderline among patients stratified by PSA level (D).

CONCLUSION

Metastatic indices were derived from MATV analysis of ^{18}F-fluorocholine PET/CT data and preliminarily found to be predictive of OS in patients with CRPC. The clinical utility of ^{18}F-fluorocholine PET/CT as a prognostic marker will need to be further established in larger studies and validated in the context of other biomarkers for advanced prostate cancer.

DISCLOSURE

The costs of publication of this article were defrayed in part by the payment of page charges. Therefore, and solely to indicate this fact, this article is hereby marked "advertisement" in accordance with 18 USC section 1734. This work was supported by United States National Institutes of Health–National Cancer Institute grant R21CA139687-02. This work does not necessarily reflect the views or opinions of The Queen's Medical Center. No other potential conflict of interest relevant to this article was reported.

REFERENCES

1. Brawley OW. Prostate cancer epidemiology in the United States. *World J Urol.* 2012;30:195–200.
2. Tannock IF, de Wit R, Berry WR, et al. Docetaxel plus prednisone or mitoxantrone plus prednisone for advanced prostate cancer. *N Engl J Med.* 2004;351:1502–1512.
3. Petrylak DP, Tangen CM, Hussain MH, et al. Docetaxel and estramustine compared with mitoxantrone and prednisone for advanced refractory prostate cancer. *N Engl J Med.* 2004;351:1513–1520.
4. Loblaw DA, Walker-Dilks C, Winquist E, Hotte SJ. Systemic therapy in men with metastatic castration-resistant prostate cancer: a systematic review. *Clin Oncol (R Coll Radiol).* 2013;25:406–430.
5. Scher HI, Halabi S, Tannock I, et al. Design and end points of clinical trials for patients with progressive prostate cancer and castrate levels of testosterone: recommendations of the Prostate Cancer Clinical Trials Working Group. *J Clin Oncol.* 2008;26:1148–1159.
6. Bubley GJ, Carducci M, Dahut W, et al. Eligibility and response guidelines for phase II clinical trials in androgen-independent prostate cancer: recommendations from the Prostate-Specific Antigen Working Group. *J Clin Oncol.* 1999;17:3461–3467.
7. Smaletz O, Scher HI, Small EJ, et al. Nomogram for overall survival of patients with progressive metastatic prostate cancer after castration. *J Clin Oncol.* 2002;20:3972–3982.
8. Halabi S, Small EJ, Kantoff PW, et al. Prognostic model for predicting survival in men with hormone-refractory metastatic prostate cancer. *J Clin Oncol.* 2003;21:1232–1237.
9. Bauman G, Belhocine T, Kovacs M, Ward A, Beheshti M, Rachinsky I. ^{18}F-fluorocholine for prostate cancer imaging: a systematic review of the literature. *Prostate Cancer Prostatic Dis.* 2012;15:45–55.
10. Price DT, Coleman RE, Liao RP, Robertson CN, Polascik TJ, DeGrado TR. Comparison of [^{18}F]fluorocholine and [^{18}F]fluorodeoxyglucose for positron emission tomography of androgen dependent and androgen independent prostate cancer. *J Urol.* 2002;168:273–280.
11. Umbehr MH, Muntener M, Hany T, Sulser T, Bachmann LM. The role of ^{11}C-choline and ^{18}F-fluorocholine positron emission tomography (PET) and PET/CT in prostate cancer: a systematic review and meta-analysis. *Eur Urol.* 2013;64:106–117.
12. Larson SM, Erdi Y, Akhurst T, et al. Tumor treatment response based on visual and quantitative changes in global tumor glycolysis using PET-FDG imaging: the visual response score and the change in total lesion glycolysis. *Clin Positron Imaging.* 1999;2:159–171.
13. Lim R, Eaton A, Lee NY, et al. ^{18}F-FDG PET/CT metabolic tumor volume and total lesion glycolysis predict outcome in oropharyngeal squamous cell carcinoma. *J Nucl Med.* 2012;53:1506–1513.
14. Van de Wiele C, Kruse V, Smeets P, Sathekge M, Maes A. Predictive and prognostic value of metabolic tumour volume and total lesion glycolysis in solid tumours. *Eur J Nucl Med Mol Imaging.* 2013;40:290–301.
15. Lim J, Dorman E, Cabral C. Automated production of [^{18}F]FECh and [^{18}F]FCH: preparation and use of [^{18}F]fluoroalkane sulfonates and fluoroalkylation agents [abstract]. *J Labelled Comp Radiopharm.* 2003;46(suppl):S46.
16. Sabbatini P, Larson SM, Kremer A, et al. Prognostic significance of extent of disease in bone in patients with androgen-independent prostate cancer. *J Clin Oncol.* 1999;17:948–957.
17. Berruti A, Tucci M, Mosca A, et al. Predictive factors for skeletal complications in hormone-refractory prostate cancer patients with metastatic bone disease. *Br J Cancer.* 2005;93:633–638.
18. Ulmert D, Kaboteh R, Fox JJ, et al. A novel automated platform for quantifying the extent of skeletal tumour involvement in prostate cancer patients using the bone scan index. *Eur Urol.* 2012;62:78–84.
19. Contractor KB, Kenny LM, Stebbing J, et al. Biological basis of [^{11}C]choline-positron emission tomography in patients with breast cancer: comparison with [^{18}F]fluorothymidine positron emission tomography. *Nucl Med Commun.* 2011;32:997–1004.
20. Ramírez de Molina A, Rodriguez-Gonzalez A, Gutierrez R, et al. Overexpression of choline kinase is a frequent feature in human tumor-derived cell lines and in lung, prostate, and colorectal human cancers. *Biochem Biophys Res Commun.* 2002;296:580–583.
21. Jiménez B, del Peso L, Montaner S, Esteve P, Lacal JC. Generation of phosphorylcholine as an essential event in the activation of Raf-1 and MAP-kinases in growth factors-induced mitogenic stimulation. *J Cell Biochem.* 1995;57:141–149.
22. Yalcin A, Clem B, Makoni S, et al. Selective inhibition of choline kinase simultaneously attenuates MAPK and PI3K/AKT signaling. *Oncogene.* 2010;29:139–149.
23. Chen J, Zhao Y, Li X, et al. Imaging primary prostate cancer with ^{11}C-choline PET/CT: relation to tumour stage, Gleason score and biomarkers of biologic aggressiveness. *Radiol Oncol.* 2012;46:179–188.
24. Glunde K, Ackerstaff E, Mori N, Jacobs MA, Bhujwalla ZM. Choline phospholipid metabolism in cancer: consequences for molecular pharmaceutical interventions. *Mol Pharm.* 2006;3:496–506.
25. Roedl JB, Colen RR, Holalkere NS, Fischman AJ, Choi NC, Blake MA. Adenocarcinomas of the esophagus: response to chemoradiotherapy is associated with decrease of metabolic tumor volume as measured on PET-CT—comparison to histopathologic and clinical response evaluation. *Radiother Oncol.* 2008;89:278–286.
26. Chen HH, Chiu NT, Su WC, Guo HR, Lee BF. Prognostic value of whole-body total lesion glycolysis at pretreatment FDG PET/CT in non-small cell lung cancer. *Radiology.* 2012;264:559–566.
27. Sartor AO, Tangen CM, Hussain MH, et al. Antiandrogen withdrawal in castrate-refractory prostate cancer: a Southwest Oncology Group trial (SWOG 9426). *Cancer.* 2008;112:2393–2400.
28. Mulders PF, Schalken JA. Measuring therapeutic efficacy in the changing paradigm of castrate-resistant prostate cancer. *Prostate Cancer Prostatic Dis.* 2009;12:241–246.
29. McCarthy M, Siew T, Campbell A, et al. ^{18}F-fluoromethylcholine (FCH) PET imaging in patients with castration-resistant prostate cancer: prospective comparison with standard imaging. *Eur J Nucl Med Mol Imaging.* 2011;38:14–22.

The Journal of NUCLEAR MEDICINE

Prognosis Related to Metastatic Burden Measured by ^{18}F-Fluorocholine PET/CT in Castration-Resistant Prostate Cancer

Sandi A. Kwee, John Lim, Alex Watanabe, Kathleen Kromer-Baker and Marc N. Coel

J Nucl Med. 2014;55:905-910.
Published online: March 27, 2014.
Doi: 10.2967/jnumed.113.135194

The Journal of Nuclear Medicine is published monthly.
SNMMI | Society of Nuclear Medicine and Molecular Imaging
1850 Samuel Morse Drive, Reston, VA 20190.
(Print ISSN: 0161-5505, Online ISSN: 2159-662X)

SNMMI SOCIETY OF NUCLEAR MEDICINE AND MOLECULAR IMAGING